Light-Harvesting in Carbonyl-Terminated Phenylacetylene Dendrimers: The Role of Delocalized Excited States and the Scaling of Light-Harvesting Efficiency with Dendrimer Size†

Tai Sang Ahn,‡ Alexis L. Thompson,§ P. Bharathi,§ Astrid Müller,‡ and Christopher J. Bardeen*,‡

Department of Chemistry, University of California, Riverside, Riverside, California 92521, and Department of Chemistry, University of Illinois, Urbana−Champaign, 600 South Mathews Avenue, Urbana, Illinois 61801

Received: November 24, 2005; In Final Form: February 10, 2006

The photophysics of a family of conjugated phenylacetylene (PA) light-harvesting dendrimers are studied using steady-state and time-resolved optical spectroscopy. The dendrimers consist of a substituted PA core surrounded by meta-branched PA arms. The total number of PA moieties ranges from 3 (first generation) to 63 (fifth generation). By using an alcohol/ketone substituent at the dendrimer core, we avoid through-space Forster transfer from the peripheral PA donors to the core acceptor (in this case, the carbonyl group), which simplifies the analysis of these molecules relative to the perylene-terminated molecules studied previously. The delocalized excited states previously identified in smaller dendrons are seen in these larger dendrimers as well, and their influence on the intersite electronic energy transfer (EET) is analyzed in terms of a point-dipole Forster model. We find that these new delocalized states can both enhance EET (by decreasing the spatial separation between donor and acceptor) and degrade it (by lowering the emission cross section and shifting the energy, resulting in poorer spectral overlap between donor and acceptor). The combination of these two effects leads to a calculated intersite transfer time of 6 ps, in reasonable agreement with the 5−17 ps range obtained from experiment. In addition to characterizing the electronic states and intersite energy transfer times, we also examine how the overall light-harvesting efficiency scales with dendrimer size. After taking the size dependence of other nonradiative processes, such as excimer formation, into account, the overall dendrimer quenching rate k_Q is found to decrease exponentially with dendrimer size over the first four generations. This exponential decrease is predicted by simple theoretical considerations and by kinetic models, but the dependence on generation is steeper than expected based on those models, probably due to increased disorder in the larger dendrimers. We discuss the implications of these results for dendrimeric light-harvesting structures based on PA and other chemical motifs.

Introduction

Dendrimer molecules represent a fast-growing field of research in macromolecular organic chemistry. Their multigenerational branched architecture allows the synthetic chemist to associate an exponentially growing number of active units around a central chemical group located at the core of the dendrimer. If the active units are conjugated molecules that absorb light and the core is an energy acceptor or trap, then such dendrimers can be used as light-harvesters,[1] in analogy to natural photosynthetic systems.[2,3] Such systems have received considerable attention as light-harvesting elements for solar energy conversion. The goal is to build a molecule with a huge effective absorption cross section, where the initially absorbed energy is then transferred from the peripheral donors to the acceptor (trap) at the base of the dendrimer. Many variants of light-harvesting architectures have been constructed, and their electronic energy transfer (EET) dynamics have been studied, ranging from all-conjugated networks based on phenylacetylene,[4−7] phenylene-vinylene,[8] and phenylene linkers[9] to networks of conjugated molecules (porphyrins,[10−13] perylenes,[14,15] and other organic dyes) linked by nonconjugated groups such as benzyl-ethers[16−22] and amines.[23,24] In addition to varying the chemical nature of the dendrimer subunits and linker groups, researchers have also manipulated the energetic structure of these molecules. For example, several researchers have built energy gradients into their dendrimers to funnel the energy to the core more efficiently.[4,25,26]

While synthetic dendrimers clearly hold much promise as light-harvesters, there are some outstanding questions in terms of how to design an optimal synthetic light-harvesting molecule. One important question concerns the practical limitations on dendrimer size. For any dendrimer structure, there will be a size limit beyond which an excitation starting at the outer layer of donors will fail to reach the core acceptor. How quickly this limit is reached depends on how the light-harvesting efficiency scales with dendrimer size. A second issue concerns the chemical details of the dendrimer structure. While the entirely conjugated dendrimers and those consisting of chromophores attached by nonconjugated linkers share the same overall architecture, there are important differences. If nonconjugated linkers separate the electronic wave functions of adjacent chromophores, then the electronic structure of these molecules is very similar to that of the isolated chromophores in solution. This lack of extended electronic states makes it possible to understand the energy transfer dynamics in terms of through-space Forster interactions. Electronic energy transfer in this type of dendrimer has been analyzed quantitatively using a combination of Forster theory and a computational analysis of the dendrimer conformations.[27] Fully conjugated dendrimers, on the other hand, have the advantage that they have a higher net density of chromo-

† Part of the special issue "Charles B. Harris Festschrift".

* Author to whom correspondence should be addressed. E-mail: christopher.bardeen@ucr.edu.

‡ University of California, Riverside.

§ University of Illinois, Urbana−Champaign.

10.1021/jp056831e CCC: $33.50
Published on Web 05/28/2006

phores, since no atoms are used solely as linkers. A second possible advantage is that electronic communication between chromophores can lead to extended electronic states and coherent transfer[28] or enhanced through-bond energy transfer.[29−32]

In this paper, we focus on the two issues raised in the preceding paragraph in the context of a specific chemical system, namely, conjugated PA dendrimers. We concentrate on EET through a network of isoenergetic PA-based monodendrons rather than energy cascade dendrimers. While energy gradients increase the efficiency of EET to the core, they do so at an energetic cost. The exciton loses energy at every step down the cascade, so the energy available when it reaches the core is less than when it started at the periphery. Thus while the efficiency of an excitation reaching the core may be 100%, that excitation may only have 75% of the original photon energy. This type of energy loss is in addition to the inevitable energy loss due to vibrational relaxation in the excited electronic state, which is reflected in the broad spectra and Stokes shift in the condensed phase, and typically is 5−10% of the photon energy at the absorption maximum. Besides avoiding energy losses due to cascading energy levels, the isoenergetic motif is also the simplest to analyze, being characterized by a single intersite transfer time rather than multiple transfer rates. We have synthesized the PA dendrimer structures originally studied by Devadoss et al.,[4] but substituting an acetophenone group for the original perylene acceptor. The carbonyl facilitates rapid intersystem crossing when the attached PA segment is in its excited state, making it an effective fluorescence quencher. This ketone moiety on the core PA group acts as a dark quencher, essentially eliminating the possibility of through-space Forster energy transfer from the dendrimer arms to the core acceptor, which was assumed to be the dominant mode of EET in the original perylene-terminated compounds.[4,33−37] In addition, by reducing the ketone to an alcohol, we can turn off the fluorescence quenching. By using this series of PA dendrimers, whose structures are given in Figure 1, we can determine how the intrinsic light-harvesting efficiency decreases as the dendrimer generation is increased and how the efficiency is impacted by the nature of the electronic states involved in the EET. We examine various types of size-dependent effects in these monodendrons, all of which affect the light-harvesting efficiency. We find that low-energy excimer-like states become more prevalent in the higher generation dendrimers, and these species compete with singlet EET to the core acceptor. In principle, however, excimer formation can be prevented by appropriate chemical substitution to sterically hinder close approach of the aromatic groups. Other nonradiative relaxation processes also become enhanced in larger monodendrons due to steric effects or nonemissive aggregate formation. Once these processes are accounted for, the intrinsic quenching rate still depends on dendrimer size simply due to the fact that in larger dendrimers the excitation has more difficulty finding the trap as it diffuses through the donor network. In this work, we find that this intrinsic quenching rate decreases exponentially with generation, as predicted on the basis of simple theoretical considerations. In terms of the electronic states of these branched molecules, we confirm that the delocalized excited states observed previously in smaller dendrons[38,39] also play a role in the larger structures used for light-harvesting. In addition, we evaluate the implications of these states for the intersite energy transfer, which occurs on a time scale of 5−17 ps in these molecules. Using a point-dipole Forster model to interpret our results, we find that the extended nature of the delocalized excited state at least partially compensates for the loss of spectral overlap due to its red-shifted emission. Our work provides a good illustration of how the properties of these large molecules depend both on chemical connectivity within the dendrimer and on its overall size. In terms of their photophysical properties, PA dendrimers cannot be regarded merely as geometrical collections of diphenylacetylene (DPA) monomers. Instead, from the nature of their quantum states to how their efficiency scales with size, they possess unique properties that can both enhance and degrade their performance as light-harvesters.

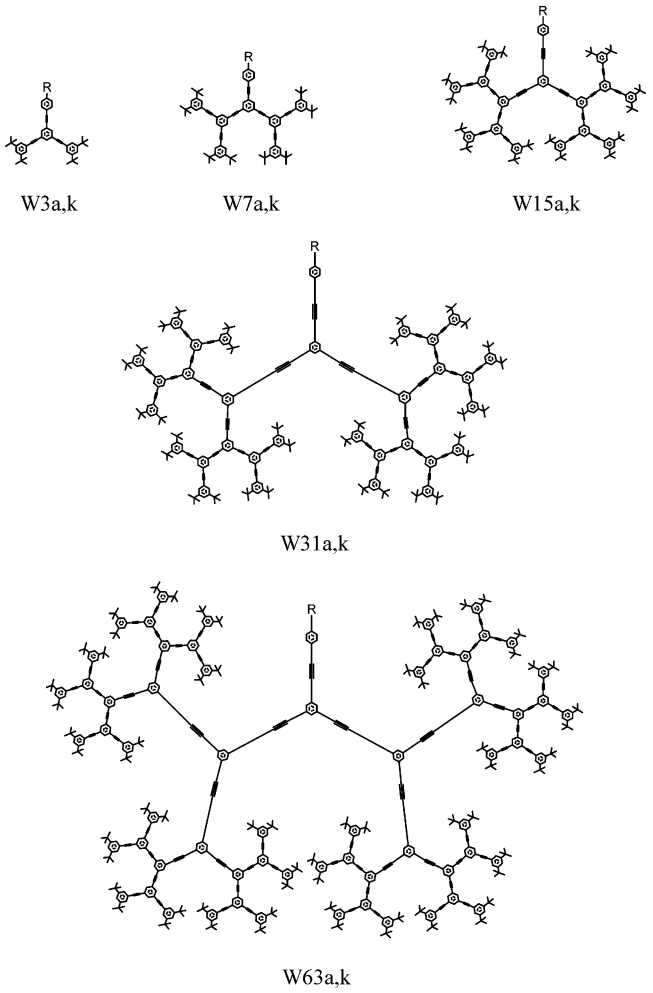

a: R = $CHOH(CH_3)$
k: R = $CO(CH_3)$

Figure 1. Structures of PA dendrimers studied in this work.

Experimental Section

The dendrimers are synthesized in a manner similar to that reported earlier,[4,40] and details of the synthetic method, product characterization, and yields can be found in the Supporting Information.

Cyclohexane is used as the solvent for all absorption and fluorescence measurements. Steady-state absorption and fluorescence spectra are recorded on a Varian Cary 50 UV−vis spectrophotometer and a Spex Fluorolog fluorometer, respectively. To obtain quantum yield values, four different concentrations of each molecule were prepared, along with two standards (perylene and anthracene), all with concentrations resulting in peak absorbance values below 0.12 to avoid self-absorption effects. The quantum yields are obtained relative to both anthracene[41] or perylene,[42] which gave similar values after applying correction factors for the different solvent refractive indices.[43] Changing the sample concentration had no effect on the spectral shapes or time-resolved fluorescence data, which

rules out the role of aggregates in the spectroscopy. This ability of the carbonyl group to quench the PA fluorescence is confirmed by fluorescence experiments on 4′-phenylethynylacetophenone, whose fluorescence quantum yield was found to be less than 0.001.

Excitation pulses for picosecond time-resolved emission measurements are generated using a home-built noncollinear optical parametric amplifier (NOPA) pumped by the 800 nm output of a 40 kHz Spectra Physics Spitfire regenerative amplifier. For these measurements, the 600 nm NOPA output is frequency-doubled to generate the 300 nm excitation beam using a 0.4 mm β-barium borate (BBO) crystal. The fluorescence is collected perpendicular to the excitation beam, collimated, and focused into a Spectra Pro-150 spectrometer with a 150 grooves/mm grating to disperse the spectrum before being passed to a Hamamatsu C4334 streak camera. The instrumental response time of this instrument is ~15 ps in a 1 ns sweep window, and the spectral resolution is 2.5 nm.

The fluorescence spectra of W31k, W63a, and W63k all show the appearance of broad, red-shifted emission, which likely originates from an excimer state. The fluorescence from these compounds 10 ns after the excitation pulse is dominated by this excimer emission. For these molecules, we have to separate the contribution of the singlet and excimer emissions to obtain the quenching rate of the singlet by itself. To do this, the steady-state emission spectra and the time-resolved emission spectra at each time interval are least-squares fitted to a weighted sum of monomer and excimer spectra[44]

$$S(\lambda,t) = a_m(t)S_m(\lambda) + a_e(t)S_e(\lambda) \quad (1)$$

where $S(\lambda,t)$ is the measured fluorescence signal and $S_m(\lambda)$ and $S_e(\lambda)$ are the fluorescence spectra of the singlet and excimer, respectively, with $a_m(t)$ and $a_e(t)$ as their coefficients. The fluorescence spectra of the initially excited singlet state is assumed to match the spectrum of W7a, a molecule that does not show any excimer emission. The excimer spectrum is taken to be the fluorescence spectrum measured after a 10 ns delay, and this spectrum varies slightly from molecule to molecule. The singlet fluorescence quantum yield of the monomer is obtained by multiplying the total fluorescence quantum yield by the percentage of the steady-state fluorescence signal due to the monomer alone. The time evolution of coefficient $a_m(t)$ in fluorescence lifetime measurements is taken as the decay of the monomer fluorescence.

Many workers have developed theoretical models for both the energy transfer kinetics[45−49] and the electronic states of dendrimers.[50,51] To numerically model the EET in the dendrimers, we use a relatively simple kinetic model involving only incoherent nearest-neighbor transfer, which resulted in a set of coupled linear differential equations. This model is similar to Pauli master equation approaches used previously to model light-harvesting systems,[52,53] and a schematic outline of this model applied to the W7k dendrimer is given in Figure 2. The resulting matrix of seven differential equations is given by

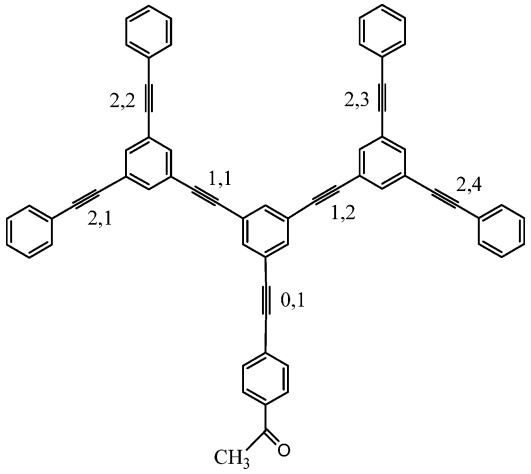

Figure 2. Schematic outline of calculation model applied to W7k dendrimer. The index 0,1 denotes the trap chromophore, while 1,1 denotes chromophore 1 in the first generation.

This set of coupled linear differential equations is solved numerically using MATLAB ode45 routines for different initial conditions that involve the excitation starting at the first (1,x) or second (2,x) layer of donor chromophores. For all dendrimers, we find that the trapping kinetics, as measured by the growth in population of the trapping site, after a weighted average over all initial conditions, are well-described by a single exponential. This overall quenching process is then characterized by a single rate constant k_Q. It is straightforward to extend the model to larger dendrimers and examine how the total quenching rate depends on k_{EET} and on the generation N.

Results and Discussion

Steady-State and Time-Resolved Spectroscopy. Figure 3 shows the absorption and fluorescence spectra of the W15a and W15k alcohol- and ketone-terminated dendrimers. These spectra are representative of the entire PA family of compounds used in this work. Both W15a and W15k have the characteristic PA absorption peaked at around 310 nm, with a broad progression of multiple peaks extending to shorter wavelengths. The W15k molecule has a slight shoulder to the long wavelength side of the absorption, due to the carbonyl n $\rightarrow \pi^*$ transition, which is not present in the alcohol. In addition, the W15k fluorescence spectrum is slightly broadened relative to that of W15a. This broadening of the fluorescence spectrum in both the ketones and the alcohols becomes more pronounced as the dendrimer size increases. But the broadened emission is not the result of a separate emitting species in the smaller dendrimers, since the fluorescence spectrum remains constant with time delay (see below). Only in the larger dendrimers do we see clear evidence for a second fluorescent species. Figure 4 shows the fluorescence spectra of molecules W15a, W31a, and W63a in cyclohexane. In comparison to W15a, W31a exhibits a slight broadening of

$$\frac{\partial}{\partial t}\begin{bmatrix} N_{trap} \\ N_{1,1} \\ N_{1,2} \\ N_{2,1} \\ N_{2,2} \\ N_{2,3} \\ N_{2,4} \end{bmatrix} = \begin{bmatrix} 0 & k_{trap} & k_{trap} & 0 & 0 & 0 & 0 \\ 0 & -(k_f + k_{trap} + 3k_{EET}) & k_{EET} & k_{EET} & k_{EET} & 0 & 0 \\ 0 & k_{EET} & -(k_f + 2k_{EET}) & 0 & 0 & k_{EET} & k_{EET} \\ 0 & k_{EET} & 0 & -(k_f + k_{trap} + 3k_{EET}) & k_{EET} & 0 & 0 \\ 0 & k_{EET} & 0 & k_{EET} & -(k_f + 2k_{EET}) & 0 & 0 \\ 0 & 0 & k_{EET} & 0 & 0 & -(k_f + 2k_{EET}) & k_{EET} \\ 0 & 0 & k_{EET} & 0 & 0 & k_{EET} & -(k_f + 2k_{EET}) \end{bmatrix} \begin{bmatrix} N_{trap} \\ N_{1,1} \\ N_{1,2} \\ N_{2,1} \\ N_{2,2} \\ N_{2,3} \\ N_{2,4} \end{bmatrix} \quad (2)$$

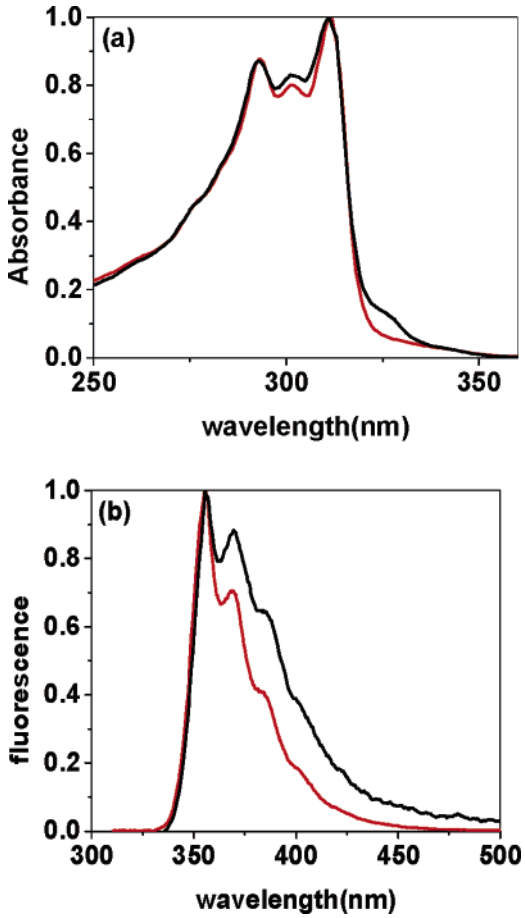

Figure 3. Normalized steady-state absorption **(**a**)** and emission **(**b**)** spectra for alcohol-terminated W15a (red line) and ketone-terminated W15k (black line).

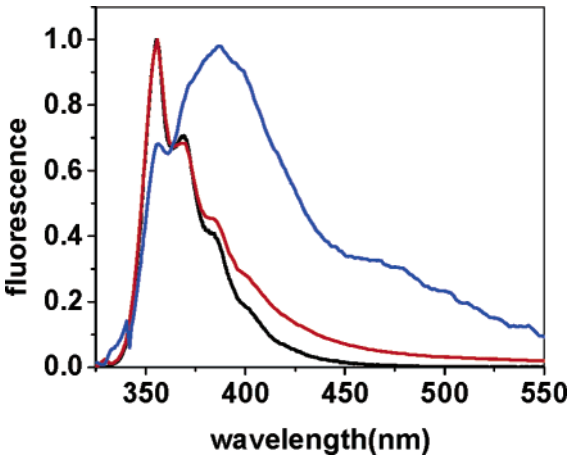

Figure 4. Normalized fluorescence spectra of alcohol-terminated dendrimers W15a (black line), W31a (red line), and W63a (blue line) in cyclohexane.

the emission beginning at around 400 nm. In W63a, this broadening is replaced by a pronounced peak centered at 400 nm that now accounts for the bulk of the emission. The presence of the alcohol group has a minimal effect on dendrimers W3a−W31a, since their fluorescence lifetimes and quantum yields in Table 1 are within 10−20% of those measured for the phenyl-terminated molecules studied previously by ourselves and Devadoss et al.[4,39] The quantum yield of W63a is significantly lower than the corresponding phenyl-terminated dendrimer,

TABLE 1: Photophysical Parameters for PA Alcohol-Terminated Dendrimers[a]

	fluorescence lifetimes (ns) and coefficients				$\langle\tau_{fl}\rangle$	quantum	k_{nr}	%	
	A_1	τ_1	A_2	τ_2	(ns)	yield	(ns^{-1})	excimer	R^2 [c]
W3a	1	10.8			10.8	0.35	0.061	0	0.996
W7a	1	10.1			10.1	0.33	0.067	0	0.997
W15a	1	9.2			9.2	0.30	0.077	0	0.998
W31a	0.31	1.6	0.69	8.3	6.2	0.16	0.13	0	0.996
W63a[b]	0.56	0.3	0.44	1.0	0.6	0.009	1.6	78	0.984

[a] Average fluorescence lifetime, $\langle\tau_{fl}\rangle$, for biexponential decays were calculated using the formula, $\langle\tau_{fl}\rangle = (A_1\tau_1 + A_2\tau_2)/(A_1 + A_2)$. Nonradiative decay rates, k_{nr}, for the excited electronic state of dendrimers were calculated using the formula, $k_{nr} = 1/\tau_{rad} - 1/\langle\tau_{fl}\rangle$, where $\tau_{rad} = 31 \pm 2$ ns. [b] This dendrimer contains excimer emission. Excimer removed emission data were used for fluorescence lifetime and quantum yield analysis. [c] R^2 is the square of the correlation coefficient R, as used in standard statistics.

however, suggesting a larger perturbation by the alcohol moiety in this molecule. If we use CH_2Cl_2 as a solvent, then the 400 nm peak in W63a is reduced by approximately 30%, and the emission more closely resembles that of W31a. The broad emission at 400 nm is indicative of PA excimer formation and has been used as a way to monitor folding transitions in various types of PA oligomers.[54] Through the use of such oligomers, it has been shown that CH_2Cl_2 is the best "unfolding"solvent for this class of molecules.[55] This is consistent with our observation that the excimer emission is diminished in this solvent. A second possible explanation for the lack of excimer emission in CH_2Cl_2 is that the solvent halogen atoms preferentially quench the excimer through a heavy atom effect.[56]

Figure 5a shows the normalized fluorescence decays for molecules W3a, W7a, W15a, and W31a in cyclohexane. While the decays appear single-exponential during the first few nanoseconds, in the two largest dendrimers there is a second, longer-lived component, as summarized in Table 1. The biexponential decays are indicative of the coexistence of at least two types of fluorescing species in the larger dendrimers. The fluorescence decays for the ketone-terminated dendrimers are shown in Figure 5b and are much more rapid than the decays of the alcohol-terminated dendrimers. The decays of W15k, W31k, and W63k are biexponential as well, indicating the presence of multiple species. An obvious candidate for the long-lived emissive species is the excimer emission identified in Figure 4, and indeed Figure 6 shows that the 400 nm excimer emission comprises a significant portion of the later emission from W31k, for example. But we find that excimer formation is not by itself sufficient to reproduce the observed biexponential decays and increase in k_{nr}. Even in the absence of a discernible excimer contribution, the singlet emission decays in some of the larger dendrimers (W31a, W15k) still required a biexponential to adequately fit the data.

Tables 1 and 2 summarize the steady-state and time-resolved spectroscopic properties for both the alcohol- and the ketone-terminated dendrimers. If we turn our attention first to the nature of the singlet emission peaked at 360 nm, we can make two observations. First, in all the dendrimers studied, the shape and position of the fluorescence overlaps that of the tri-ethynylbenzene fragment studied in our previous work. This fact is emphasized in Figure 7, where the spectra of the mono-, di-, and tri-phenylethynylene benzenes are plotted, along with that of W15a. In addition to the identical fluorescence spectra, the dendrimers also have a similar radiative lifetime to the dendron. For the biexponential decays, we have defined $\langle\tau_{fl}\rangle$, the weighted

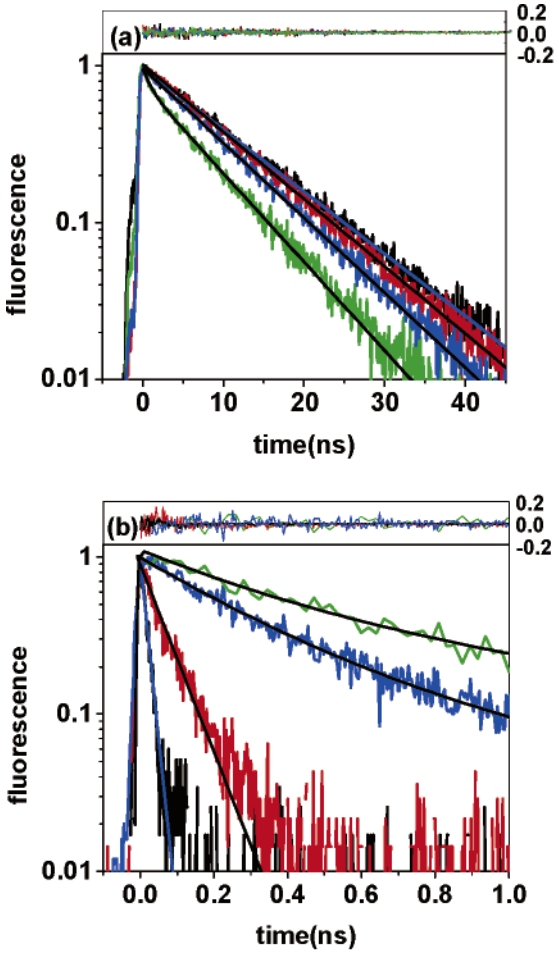

Figure 5. Normalized fluorescence decays **(a)** for alcohol-terminated dendrimers W3a (black line), W7a (red line), W15a (blue line), and W31a (green line) and **(b)** for ketone-terminated dendrimers W3k (black line), W7k (red line), W15k (blue line), and W31k (green line) in cyclohexane at room temperature along with the fits for W7, W15, and W31 (black line) and W3 (blue line). The residuals on top of the graph are plotted in the same colors as the decays. Note the different time axes in the figures.

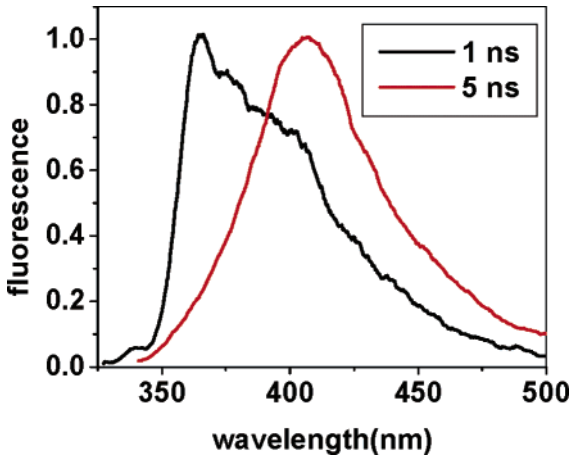

Figure 6. Early (1 ns, black line) and later (5 ns, red line) emission spectra of the ketone-terminated dendrimer W31k.

average of the fluorescence decay times, as

$$\langle \tau_{fl} \rangle = \frac{A\tau_A + B\tau_B}{A + B} \tag{3}$$

where A and B are the amplitudes of the two decays. It is straightforward to show that this single parameter is directly related to the fluorescence quantum yield ϕ as given in the following equation

$$\phi = \frac{\langle \tau_{fl} \rangle}{\tau_{rad}} \tag{4}$$

where τ_{rad} is the radiative lifetime. Figure 8 plots the fluorescence quantum yields versus the average fluorescence lifetimes, which are given in Table 1. To extract quantum yields for the singlet state only, we need to separate the singlet and excimer contributions to the steady-state and time-resolved fluorescence signals for W63a, as detailed in the Experimental Section. If all the dendrimers have the same τ_{rad}, then eq 4 predicts that a plot of ϕ versus $\langle \tau_{fl} \rangle$ should yield a straight line with a slope of $1/\tau_{rad}$. Indeed, this is what is observed, and the slope obtained from a linear least-squares fit to the data yields $\tau_{rad} = 31 \pm 2$ ns, which lies between the values of 28 and 43 ns obtained for the di- and tri-phenylethynyl-benzene molecules, respectively. This relatively long value for τ_{rad} is consistent with the delocalized state observed previously in the smaller dendrons.[38]

TABLE 2: Photophysical Parameters for PA Ketone-Terminated Dendrimers as Defined in the Text

	fluorescence lifetimes (ns) and coefficients						
	A_1	τ_1	A_2	τ_2	$\langle \tau_{fl} \rangle$ (ns)	$k_Q = 1/\langle \tau_{fl}^{ket} \rangle - 1/\langle \tau_{fl}^{alc} \rangle$ (ns^{-1})	R^2
W3k	1	0.017			0.017	58	0.978
W7k	1	0.08			0.08	12	0.970
W15k	0.52	0.18	0.48	0.66	0.41	2.3	0.980
W31k*	0.34	0.29	0.66	1.2	0.9	0.94	0.984
W63k*	0.68	0.20	0.32	0.61	0.33	3.0	0.986

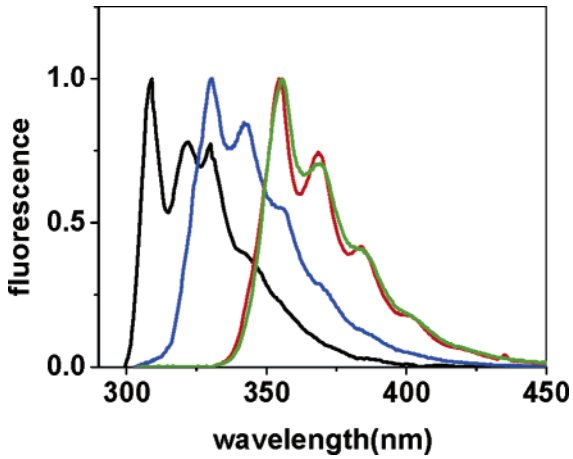

Figure 7. Normalized steady-state fluorescence spectra of the mono- (black line), di- (blue line), and tri- (red line) phenylethynylene benzenes and the alcohol-terminated dendrimer W15a (green line).

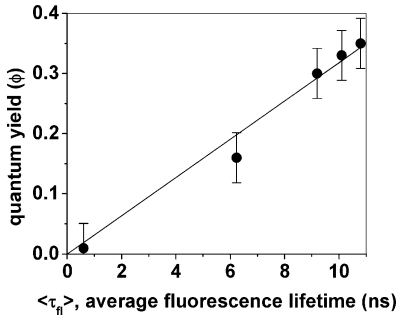

Figure 8. Plot of fluorescence quantum yields versus the average fluorescence lifetimes $\langle \tau_{fl} \rangle$ of W3a, W7a, W15a, W31a, and W63a in cyclohexane. The slope of this line yields a $\tau_{rad} = 31 \pm 2$ ns.

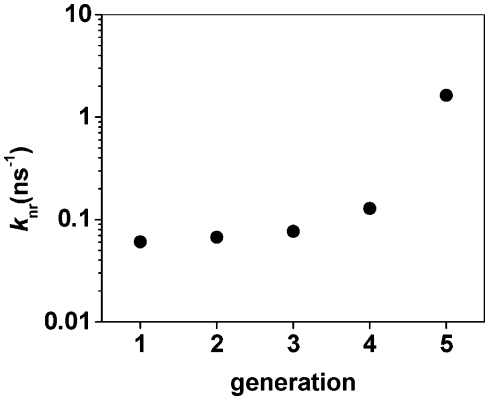

Figure 9. Nonradiative decay rate, k_{nr}, for the excited electronic state of dendrimer versus dendrimer size (in units of generation) for W3a through W63a.

For comparison, if the emitting state were localized on a diphenylacetylene segment, then τ_{rad} would be expected to be similar to that of DPA, which is more than an order of magnitude shorter, 1.2 ns.[38,57] The τ_{rad} value for the dendrimers is shorter than that of the tri-phenylethynyl-benzene, despite the similarity of the fluorescence spectra, and this may be due to a slight local field enhancement of the emission oscillator strength by the local dielectric of the dendrimer.[58,59] We should note that although analysis of our data gives similar τ_{rad} values for all the alcohol dendrimers, this was not the case for the phenyl-terminated dendrimers previously studied by Devadoss et al., where the calculated τ_{rad} ranged from 12 to 32 ns with no apparent trend.[4] The reasons for this discrepancy are unclear. The important point is that our data are consistent with the dendrimer excited state being centered on a tri-ethynyl-benzene group, rather than on the acetylene bond, and which is slightly delocalized into the surrounding carbon−carbon triple bonds.

While the radiative lifetime is essentially independent of dendrimer size, the nonradiative rate k_{nr} increases dramatically with dendrimer size. The general definition of k_{nr} is given by

$$k_{nr} = \frac{1}{\langle \tau_{fl} \rangle} - \frac{1}{\tau_{rad}} \tag{5}$$

where τ_{rad} is set to 31 ns as indicated by the data in Figure 8. Figure 9 plots k_{nr} versus dendrimer size for W3a through W63a. There is a clear increase in the nonradiative decay with size, some of which may be attributed to the increasing conformational flexibility in the larger molecules. The presence of these multiexponential decays points toward the existence of multiple conformations within the molecules that affect the fluorescence lifetimes. The mechanism by which they accelerate the fluorescence decay is not known, but it should be remembered that all these PA dendrons have a dominant nonradiative decay channel, on the order of 60−70%, even in the absence of any EET or excimer formation, and it is likely that this channel is sensitive to environmental perturbations. DPA by itself has a very low fluorescence quantum yield due to rapid electronic curve crossing to a dark excited state followed by internal conversion to the ground state.[60−62] This process is very temperature-dependent and is believed to involve torsional motion of the phenyl rings.[63] If analogous types of internal conversion processes govern the nonradiative relaxation in the present family of dendrimers, then it would not be surprising that the different steric environments present in the larger, more disordered dendrimers would lead to a distribution of decay times. Of course, some of these conformations would also be expected to lead to weakly emissive states too, such as the excimer-type states we observe in the larger dendrimers. Interestingly, this excimer formation appears to be less pronounced in the phenyl-terminated dendrimers studied by Devadoss et al.[4] Enhanced emission at 400 nm has also been observed in dendrimers with methoxy substituents at the core.[64] It may be that the presence of an oxygen atom at the core is able to influence excimer formation in the larger dendrimers, possibly due to backfolding that enables peripheral PA groups and the core oxygen to come into contact. From this analysis, we see that the measured fluorescence lifetime of these PA dendrimers is determined not only by EET to the core quenching site but also by excimer formation and conformation-dependent nonradiative processes as well. To analyze the EET process through the PA network, which is the main focus of this paper, we must separate these different contributions. We will do this in the analysis below so that we may draw some conclusions about how the light-harvesting efficiency scales with dendrimer size and also how the delocalized states identified above affect the EET.

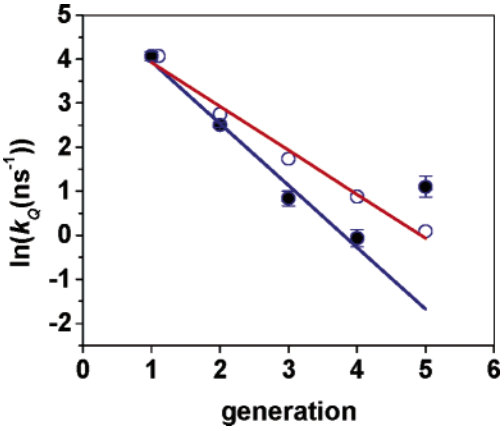

Figure 10. Experimental (●) and calculated (○) fluorescence quenching rates (ln(k_Q)) versus dendrimer size (in units of generation). The linear least-squares fit (black line) to the first four experimental points yields a slope of 1.4, while the linear least-squares fit (red line) to the five calculated points yields a slope of 1.0.

Size Dependence of Intrinsic Quenching Rate. To analyze the EET process in these molecules, we define the intrinsic quenching rate k_Q as

$$k_Q = \langle k_{fl}^{ket} \rangle - \langle k_{fl}^{alc} \rangle = \frac{1}{\langle \tau_{fl}^{ket} \rangle} - \frac{1}{\langle \tau_{fl}^{alc} \rangle} \tag{6}$$

where the brackets denote the average fluorescence decay rate, in the case of a multiexponential decay as described in the Experimental Section. This experimental quantity, which describes the quenching rate of the entire dendrimer, averaged over all generations of chromophores, is obtained after removing contributions from excimer emission from the fluorescence decays to obtain $\langle k_{fl}^{alc} \rangle$ and $\langle k_{fl}^{ket} \rangle$. The assumption is that once these contributions are removed any remaining difference between the alcohol- and the ketone-terminated dendrimer fluorescence decays is due solely to EET through the PA network to the carbonyl quencher. In Table 2, we give the experimental values obtained for k_Q for the ketone dendrimers. In Figure 10, we plot ln(k_Q) versus dendrimer size (in units of generation), along with a linear least-squares fit to the first four points. We omit the W63k point from the fit since its emission is dominated by the excimer contribution and thus its k_Q value is most affected by any error in removing that contribution. We obtain a slope of 1.4 ± 0.2. Figure 10 summarizes one of the most important results of this work: that k_Q, and thus the light-harvesting efficiency, decreases exponentially with increasing

generation. In addition to the information about the generational dependence of k_Q, the data in Table 2 and Figure 10 also provide a means to analyze k_{EET}, the intersite energy transfer rate, which indirectly determines k_Q and which will be affected by the details of the chromophore electronic structure, for example, the amount of excited-state wave function delocalization.

Given these two issues, we address the generation dependence of k_Q first. The k_Q defined in this paper is identical to the k_{ET} defined in the earlier work of Devadoss et al.[4] Using their quenching efficiency data, we can derive k_Q values for the perylene-terminated dendrimers, which are 2.26, 1.33, 5.14, 3.16, 2.27, and 1.73 ns^{-1} for dendrimers W3-per, W7-per, W15-per, W31-per, W63-per, and W127-per, respectively. There is no obvious dependence of k_Q on generation in this series of molecules. This difference between perylene- and carbonyl-terminated dendrimers may be the result of a combination of through-space Forster transfer between distant donor PA groups and the perylene, combined with some degree of backfolding of the PA arms. For example, if the PA arms in W15-per were long enough to permit the peripheral PA unit to closely approach the perylene, energy could be transferred to the core through space, skipping the intermediate PA groups. Such a scenario could explain the increase in k_Q for this molecule relative to the W7-per. The presence of multiple pathways in the perylene-terminated dendrimers makes the detailed analysis of their EET dynamics problematic. For the ketone-terminated molecules in this work, the exponential decay of k_Q with dendrimer generation can be predicted from simple geometrical considerations. If we assume that an excitation visits some fraction of available sites before trapping and that the number of available sites increases as the power of N, the generation number, we can estimate the quenching time τ_Q as being the hopping time between nearest neighbors, τ_{EET}, multiplied by the number of sites visited

$$\tau_Q \propto (\text{number of sites}) \times (\text{hopping time}) = 2^N \times \tau_{EET} \quad (7)$$

and the quenching rate is estimated to be

$$k_Q = \frac{1}{\tau_Q} \propto 2^{-N} \times k_{EET} \quad (8a)$$

$$\ln(k_Q) = -\ln(2) \times N + \ln(k_{EET}) \quad (8b)$$

Even this crude model captures the qualitative behavior of our data up to W31k. Note that eq 8b predicts a slope of $\ln(2) = 0.693$ for the data in Figure 10, as opposed to the value of 1.4 obtained experimentally. A final point is that the nearest-neighbor intersite transfer rate, k_{EET}, can also be obtained from the y-intercept of eq 8b.

To obtain a more accurate picture of the EET dynamics, we have examined the behavior of the EET and the trapping dynamics using the kinetic model outlined in the Experimental Section and eq 2. By considering only nearest-neighbor coupling and setting the trap rate $k_{trap} = k_{EET}$, we examine how k_Q scales with N, the number of generations in a given dendrimer. Our model calculates the quenching rate for a $1 \rightarrow 2$ branching dendrimer, where a single chromophore site in generation j branches out to two chromophores in generation $j + 1$. This is the situation for the PA dendrimers in this work. The calculated points are plotted along with the experimental size dependence in Figure 10. We see that the decrease in k_Q with generation is not purely exponential, although the deviation is small over this range of N. We neglect this deviation and use a linear least-squares fit to obtain a slope $m = 1.0$. The slope of this logarithmic dependence did not depend on the details of the model. For example, if we used phenyl- versus segment-centered chromophores, or added extra intragenerational coupling terms, so chromophores within a generation can transfer energy freely, no change in the slope m was observed. However, inclusion of next-nearest-neighbor coupling led to $m < 1.0$ values; i.e., the generational dependence became weaker. This is to be expected, since these terms allow the EET to skip intervening generations and make the larger dendrimers appear smaller to the traveling excitation.[65] We also examined numerically a $1 \rightarrow 3$ branching architecture, which could be obtained using a sp^3 carbon as a vertex. For this architecture, a plot of k_Q versus N leads to a slope $m = 1.4$, reflecting the more complex topology of this type of structure. Basically, as the degree of branching increases, so does the opportunity for an excitation, which begins at the dendrimer periphery, to take a wrong turn on its way to the core trapping site. Although this value agrees with that obtained experimentally, this increased branching cannot be the physical origin of the $m = 1.4$ value in our $1 \rightarrow 2$ branching molecules. An alternative way to obtain this increased density of wrong turns is to have disorder, both dynamic and static, in the model. Mukamel and co-workers have shown that energetic disorder can lead to the loss of efficient transfer in funnel-type dendrimers,[66,67] and similar effects could be operative in our molecules. As the size of the dendrimer increases, the probability of encountering a low-energy site before trapping increases as well, leading to a steeper decline in trapping efficiency than would be expected for a model where all the sites are identical. The deviation of the experimental results in Figure 10 from those of a simple calculation based on identical donor sites provides evidence that disorder, in the form of a distribution of nearest-neighbor transfer rates due to different conformations or environments, leads to a more rapid decline in k_Q. Circumstantial evidence for increasing disorder is provided by the increased excimer formation and multiexponential decays observed in the larger dendrimers. It is important to emphasize that EET can be affected by either energetic or conformational disorder. The first type affects the spectral overlap term in the Forster transfer rate, eq 9, while the second affects the orientation factor κ^2 in the same equation. The energetic disorder should also lead to inhomgeneous broadening in the steady-state absorption and fluorescence line shapes, but to reliably quantify it requires the use of nonlinear spectroscopic methods. Conformational disorder is more difficult to characterize spectroscopically, and molecular dynamics simulations are often used. Whatever the molecular origin, our results imply that the energy trapping efficiency of PA dendrimers decreases more rapidly than expected, placing an ultimate limit on the useful size of such molecules in light-harvesting applications. Of course, the absolute value of the light-harvesting efficiency will depend on the excitation lifetime and the intersite EET rates as well.

Nearest-Neighbor Intersite Transfer Rate. The second major question we need to address is the effect of the delocalized singlet state identified spectroscopically on the intersite transfer rate, k_{EET}. In principle, we can obtain this parameter from fitting our data using the kinetic models described above. Unfortunately, it is clear that those simple models do not capture the dynamics accurately, and it is likely that there is not a single value of k_{EET} that can characterize the EET dynamics of all the dendrimers in this study. Nevertheless, we can make some general statements about how the excited-state delocalization affects k_{EET}. In the W3k dendrimer, according to our model, the fluorescence quenching should reflect the single-step transfer from the first layer of chromophores to the core. Thus for this molecule, $k_Q = k_{EET}$, and we obtain a transfer time of $\sim$17 ps.

A second approach is to use eq 8b and the data in Figure 10 to extract τ_{EET} from the *y*-intercept the plot of k_Q versus generation. In this case, we obtain $k_{EET} = 5$ ps from the linear fit shown in Figure 10. Interestingly, both values are comparable to those obtained by Kleimann et al. in their studies of PA funnel dendrimers.[37] If we assume the simplest model for EET, namely, the point-dipole Forster model, then we must resolve some ambiguities concerning chromophore position and orientation. Here we will consider three different scenarios. Let us first consider the early model of these meta-coupled PA dendrimers as collections of independent DPA units that retain the spectral properties of the monomer in solution. If this were the case, we can apply the Forster formula

$$k_{ET} = \frac{1}{\tau_{fl}} \frac{R_0^6}{R^6} \tag{9a}$$

$$R_0^6 = \frac{9000\ln(10)\phi_{fl}\kappa^2}{128\pi^5 N_A n^4} \int_0^\infty \epsilon(\nu) f(\nu) \frac{d\nu}{\nu^4} = \frac{9000\ln(10)\phi_{fl}\kappa^2}{128\pi^5 N_A n^4} J \tag{9b}$$

where R is the separation between chromophores, n is the index of refraction, τ_{fl} is the fluorescence lifetime of the donor (which in this case is identical to the acceptor), ϕ_{fl} is the quantum yield, κ is an orientation factor, N_A is Avogadro's number, $\epsilon(\nu)$ is the absorption spectrum, and $f(\nu)$ is the fluorescence spectrum whose integral has been normalized to 1. R_0 combines these factors into a single length called the critical Förster radius. Note that this equation does not take static disorder effects of the type discussed in the preceding paragraph into account. If we set $\tau_{rad} = \tau_{fl}/\phi_{fl} = 1.2$ ns, $\kappa^2 = 3.06$ due to the 120° angle between the transition dipole moments which lie along the ethynyl bonds, and $\epsilon_{max} = 30\,000$ M^{-1} cm^{-1} (typical for a DPA derivative) which leads to a spectral overlap term $J = 6.8 \times 10^{17}$, we obtain $\tau_{EET} = 260$ fs. Thanks to its small Stokes shift and high oscillator strength, DPA is predicted to facilitate very rapid EET and thus would be an ideal component of a light-harvesting supermolecule. Its main drawback as a monomer is its very rapid nonradiative decay, which would effectively compete with the EET to the core. When DPA is incorporated into a covalent dendrimer, however, the spectroscopic properties of the dendron excited state change in such a way so as to inhibit EET. In the second scenario, the larger Stokes shift reduces the spectral overlap by more than an order of magnitude. If we use the absorption and emission spectra of W15k, we obtain $J = 2.5 \times 10^{16}$. Furthermore, the emission oscillator strength also decreases, with a $\tau_{rad} = 35$ ns instead of 1.2 ns. Assuming the same chromophore geometry as above, the Forster transfer time is found to be 34 ps, more than 100 times slower than what would be expected for the monomer in the same geometrical arrangement. Thus connecting the DPA subunits together in a larger conjugated structure results in lower EET efficiency than what would have been predicted based on the properties of the isolated monomer. One benefit of the new dendrimer electronic states is that the rapid internal conversion channel that quenches DPA fluorescence at room temperature appears to be eliminated. As discussed earlier, there is still a significant nonradiative relaxation process in the dendrimers, but k_{nr} is now about 1000 times slower in W3a through W31a than it is in DPA at room temperature. Another possible benefit of the dendrimer excited states is that they shift the center of the wave function from the triple bond segments to the phenyl group vertexes. If the subsequent EET event occurs between this phenyl-centered excited state and an ethynyl-centered absorbing state, then the physical separation r will be less than in the case of the ethynyl−ethynyl transfer described earlier. If we calculate the Forster rate a third time, now using $r = 3.4$ Å and $\kappa^2 = 0.67$ (assuming a randomized orientation of the phenyl-centered transition dipole due to the symmetry of the tri-ethynylphenyl group), we obtain $\tau_{EET} = 6$ ps. Thus the delocalization of the dendritic wave function to the phenyl group enhances the EET rate to an adjacent ethynylene segment by about a factor of 6.

Of course, the good agreement between the calculated value of 6 ps and the experimental value of 5−17 ps may be fortuitous. The point-dipole Forster model is known to break down at small chromophore separations and tends to overestimate the energy transfer rate in these cases. Improved models of the EET process that explicitly take into account the molecular structure and charge distribution would be expected to provide more reliable estimates of the EET rates but are beyond the scope of this paper.[68−71] A second weakness of the point-dipole model is that it only takes the through-space Coulombic interactions into account, neglecting through-bond interactions due to electron-transfer configurations.[29] Such interactions are expected to be significant in these highly conjugated systems. It may be that a cancellation of these trends (faster transfer due to through-bond effects but slower transfer due to through-space extended dipole effects) leads to the decent agreement between our calculated and experimental results. In any case, the analysis is useful to show how delocalization in these branched conjugated systems can both hinder and help intersite EET thanks to the different variables in the Forster equation. In the case of the PA dendrimers, the advantages of their compact structure and dense chromophore packing appear to be partially offset by the existence of delocalized excited states that slow the EET and prevent the achievement of the behavior predicted from the properties of the monomer alone. In the excited state, strong electronic interactions across the meta-linkages lead to a structure that, from the perspective of light-harvesting, is actually less than the sum of its parts.

Conclusion

In this work, we have characterized the spectroscopy and EET dynamics of a family of PA dendrimers. The goal was to examine the basic process of EET through the PA network by removing effects due to through-space interactions and size-dependent nonradiative relaxation processes. We found that this class of molecules has several unique photophysical properties that affect their utility as light-harvesting compounds. First, as the size of the dendrimers is increased, there is a concomitant increase in the nonradiative decay rate of the singlet state. Part of this increase is due to excimer formation in the higher generation dendrimers. The excimer acts as a long-lived trap, preventing complete energy transfer to the core. The relative importance of the excimer states depends on both the solvent and the chemical substituent at the base of the dendrimer and is most pronounced for the ketones in poor solvents. Our data on the alcohols suggests that in addition to the excimer there is at least one other nonradiative pathway that also becomes enhanced as dendrimer size increases. When these size-dependent processes are taken into account, we find that the intrinsic singlet quenching rate, k_Q, decreases exponentially with dendrimer generation and that this decrease is more rapid than expected based on simple theoretical models. The accelerated decline in k_Q most probably stems from increasing conformational disorder as the dendrimer branches are extended. The combined effects of size-dependent excimer formation, nonradiative relaxation, and disorder presents a significant barrier to scaling such structures up to even larger sizes.

In addition to evaluating how the overall light-harvesting rate changes with dendrimer size, we have also investigated the nature of the excited electronic states and their local interactions. The excited singlet state in all the PA dendrimers is consistent with the phenyl-centered state identified in earlier work on smaller PA dendrons. This state, which is shifted to lower energy and has a smaller radiative rate than that of the DPA monomer, would appear to be detrimental to energy transfer, based on a point-dipole Forster analysis. The unfavorable photophysical properties of this state can be compensated for, at least in part, by its shift in spatial position so that the phenyl-centered donor state is closer to the ethynyl-centered acceptor. Our experimental intersite transfer time of 5−17 ps is close to the 6 ps time estimated by such a model, although this agreement may be fortuitous. Our work demonstrates that the existence of such delocalized excited states must be taken into account to accurately predict the energy transfer dynamics of such conjugated structures, since a naive model based on monomeric DPA would predict intersite EET times at least an order of magnitude faster than those observed experimentally. In our model, the PA dendrimers can be thought of as hybrid energy transfer structures, in which limited delocalization is followed by through-space Coulombic transfer between the delocalized emitting states and the localized DPA acceptors.

The combination of disorder and size-dependent nonradiative decay channels, along with the evolution of new quantum mechanical states, makes the design of the conjugated supermolecules based on the PA motif a challenging problem. The potential applications of these molecules in optoelectronics provide motivation to continue to tackle these complexities. Finally, it is likely that the issues identified above will also be important for understanding the photophysics of other multichromophoric dendrimer systems.

Acknowledgment. This work was supported by the Department of Energy Grant No. DEFG-01ER15270. C.J.B. is an Alfred P. Sloan Research Fellow.

Supporting Information Available. Detailed procedure for synthesis of the keto/alcohol phenylacetylene monodendron compounds. This material is available free of charge via the Internet at http://pubs.acs.org.

References and Notes

(1) Andronov, A.; Frechet, J. M. J. *Chem. Commun.* **2000**, 1701−1710.
(2) Balzani, V.; Ceroni, P.; Maestri, M.; Vicinelli, V. *Curr. Opin. Chem. Biol.* **2003**, *7*, 657−665.
(3) Gust, D.; Moore, T. A.; Moore, A. L. *Acc. Chem. Res.* **2001**, *34*, 40−48.
(4) Devadoss, C.; Bharathi, P.; Moore, J. S. *J. Am. Chem. Soc.* **1996**, *118*, 9635−9644.
(5) Pan, Y.; Lu, M.; Peng, Z.; Melinger, J. S. *J. Org. Chem.* **2003**, *68*, 6952−6958.
(6) Pan, Y.; Peng, Z.; Melinger, J. S. *Tetrahedron* **2003**, *59*, 5495−5506.
(7) Atas, E.; Peng, Z.; Kleiman, V. D. *J. Phys. Chem. B* **2005**, *109*, 13553−13560.
(8) Meskers, S. C. J.; Bender, M.; Hubner, J.; Romanovskii, Y. V.; Oestreich, M.; Schenning, A. P. H. J.; Meijer, E. W.; Bassler, H. *J. Phys. Chem. A* **2001**, *105*, 10220−10229.
(9) Lu, D.; Feyter, S. D.; Cotlet, M.; Stefan, A.; Wiesler, U.-M.; Herrman, A.; Grebel-Koehler, D.; Qu, J.; Mullen, K.; Schryver, F. C. D. *Macromolecules* **2003**, *36*, 5918−5925.
(10) Wagner, R. W.; Johnson, T. E.; Lindsey, J. S. *J. Am. Chem. Soc.* **1996**, *118*, 1166−1180.
(11) Li, F.; Gentemann, S.; Kalsbeck, W. A.; Seth, J.; Lindsey, J. S.; Holten, D.; Bocian, D. F. *J. Mater. Chem.* **1997**, *7*, 1245−1262.
(12) Yeow, E. K. L.; Ghiggino, K. P.; Reek, J. N. H.; Crossley, M. J.; Bosman, A. W.; Schenning, A. P. H. J.; Meijer, E. W. *J. Phys. Chem. B* **2000**, *104*, 2596−2606.
(13) Choi, M.-S.; Aida, T.; Yamazaki, T.; Yamazaki, I. *Chem.—Eur. J.* **2002**, *8*, 2668−2678.
(14) Tomizaki, K.; Loewe, R. S.; Kirmaier, C.; Schwartz, J. K.; Restek, J. L.; Bocian, D. F.; Holten, D.; Lindsey, J. S. *J. Org. Chem.* **2002**, *67*, 6519−6534.
(15) Metivier, R.; Kulzer, F.; Weil, T.; Mullen, K.; Basche, T. *J. Am. Chem. Soc.* **2004**, *126*, 14634−14635.
(16) Hahn, U.; Gorka, M.; Vogtle, F.; Vicinelli, V.; Ceroni, P.; Maestri, M.; Balzani, V. *Angew. Chem., Int. Ed.* **2002**, *41*, 3595−3598.
(17) Zhou, X.; Tyson, D. S.; Castellano, F. N. *Angew. Chem., Int. Ed.* **2000**, *39*, 4301−4305.
(18) Stewart, G. M.; Fox, M. A. *J. Am. Chem. Soc.* **1996**, *118*, 4354−4360.
(19) Adronov, A.; Gilat, S. L.; Frechet, J. M. J.; Ohta, K.; Neuwahl, F. V. R.; Fleming, G. R. *J. Am. Chem. Soc.* **2000**, *122*, 1175−1185.
(20) Neuwahl, F. V. R.; Righini, R.; Adronov, A.; Malenfant, P. R. L.; Frechet, J. M. J. *J. Phys. Chem. B* **2001**, *105*, 1307−1312.
(21) Gilat, S. L.; Adronov, A.; Frechet, J. M. J. *Angew. Chem., Int. Ed.* **1999**, *38*, 1422−1427.
(22) Thomas, K. R. J.; Thompson, A. L.; Sivakumar, A. V.; Bardeen, C. J.; Thayumanavan, S. *J. Am. Chem. Soc.* **2005**, *127*, 373−383.
(23) Varnavski, O.; Samuel, I. D. W.; Palsson, L.-O.; Beavington, R.; Burn, P. L.; Goodson, T. *J. Chem. Phys.* **2002**, *116*, 8893−8903.
(24) Ranasinghe, M. I.; Varnavski, O. P.; Pawlas, J.; Hauck, S. I.; Louie, J.; Hartwig, J. F.; Goodson, T. *J. Am. Chem. Soc.* **2002**, *124*, 6520−6521.
(25) Melinger, J. S.; Pan, Y.; Kleiman, V. D.; Peng, Z.; Davis, B. L.; McMorrow, D.; Lu, M. *J. Am. Chem. Soc.* **2002**, *124*, 12002−12012.
(26) Serin, J. M.; Brousmiche, D. W.; Frechet, J. M. J. *Chem. Commun.* **2002**, 2605−2607.
(27) Maus, M.; De, R.; Lor, M.; Weil, T.; Mitra, S.; Wiesler, U.-M.; Herrmann, A.; Hofkens, J.; Vosch, T.; Mullen, K.; Schryver, F. C. D. *J. Am. Chem. Soc.* **2001**, *123*, 7668−7676.
(28) Varnavski, O. P.; Ostrowski, J. C.; Sukhomlinova, L.; Twieg, R. J.; Bazan, G. C.; Goodson, T. *J. Am. Chem. Soc.* **2002**, *124*, 1736−1743.
(29) Scholes, G. Theory of coupling in multichromophoric systems. In *Resonance Energy Transfer*; Andrews, D. L., Demidov, A. A., Eds.; Wiley: New York, 1999; pp 213−242.
(30) Scholes, G. D.; Turner, G. O.; Ghiggino, K. P.; Padden-Row, M. N.; Piet, J. J.; Schuddeboom, W.; Warman, J. M. *Chem. Phys. Lett.* **1998**, *292*, 601−606.
(31) Hsiao, J.-S.; Krueger, B. P.; Wagner, R. W.; Johnson, T. E.; Delaney, J. K.; Mauzerall, D. C.; Fleming, G. R.; Lindsey, J. S.; Bocian, D. F.; Donohoe, R. J. *J. Am. Chem. Soc.* **1996**, *118*, 11181−11193.
(32) Seth, J.; Palaniappan, V.; Wagner, R. W.; Johnson, T. E.; Lindsey, J. S.; Bocian, D. F. *J. Am. Chem. Soc.* **1996**, *118*, 11194−11207.
(33) Kopelman, R.; Shortreed, M.; Shi, Z.-Y.; Tan, W.; Xu, Z.; Moore, J. S.; Bar-Haim, A.; Klafter, J. *Phys. Rev. Lett.* **1997**, *78*, 1239−1242.
(34) Shortreed, M.; Swallen, S. F.; Shi, Z.-Y.; Tan, W.; Xu, Z.; Devadoss, C.; Moore, J. S.; Kopelman, R. *J. Phys. Chem. B* **1997**, *101*, 6318−6322.
(35) Swallen, S. F.; Kopelman, R.; Moore, J. S.; Devadoss, C. *J. Mol. Struct.* **1999**, *485−486*, 585−597.
(36) Swallen, S. F.; Zhu, Z.; Moore, J. S.; Kopelman, R. *J. Phys. Chem. B* **2000**, *104*, 3988−3995.
(37) Kleiman, V. D.; Melinger, J. S.; McMorrow, D. *J. Phys. Chem. B* **2001**, *105*, 5595−5598.
(38) Gaab, K. M.; Thompson, A. L.; Xu, J.; Martinez, T. J.; Bardeen, C. J. *J. Am. Chem. Soc.* **2003**, *125*, 9288−9289.
(39) Thompson, A. L.; Gaab, K. M.; Xu, J.; Bardeen, C. J.; Martinez, T. J. *J. Phys. Chem. A* **2004**, *108*, 671−682.
(40) Xu, Z.; Kahr, M.; Walker, K. L.; Wilkins, C. L.; Moore, J. S. *J. Am. Chem. Soc.* **1994**, *116*, 4537−4550.
(41) Melhuish, W. H. *J. Phys. Chem.* **1961**, *65*, 229−235.
(42) Murov, S. L.; Carmichael, I.; Hug, G. L. *Handbook of Photochemistry*, 2nd ed.; Marcel Dekker: New York, 1993.
(43) Demas, J. N.; Crosby, G. A. *J. Phys. Chem.* **1971**, *75*, 991−1024.
(44) Lim, S.-H.; Bjorklund, T. G.; Bardeen, C. J. *J. Phys. Chem. B* **2004**, *108*, 4289−4295.
(45) Bentz, J. L.; Hosseini, F. N.; Kozak, J. J. *Chem. Phys. Lett.* **2003**, *370*, 319−326.
(46) Bar-Haim, A.; Klafter, J.; Kopelman, R. *J. Am. Chem. Soc.* **1997**, *119*, 6197−6198.
(47) Bar-Haim, A.; Klafter, J. *J. Phys. Chem. B* **1998**, *102*, 1662−1664.
(48) Kirkwood, J. C.; Scheurer, C.; Chernyak, V.; Mukamel, S. *J. Chem. Phys.* **2001**, *114*, 2419−2429.
(49) Subramanian, V.; Evans, D. G. *J. Phys. Chem. B* **2004**, *108*, 1085−1095.
(50) Tretiak, S.; Chernyak, V.; Mukamel, S. *J. Phys. Chem. B* **1998**, *102*, 3310−3315.
(51) Poliakov, E. Y.; Chernyak, V.; Tretiak, S.; Mukamel, S. *J. Chem. Phys.* **1999**, *110*, 8161−8175.
(52) Patten, P. G. V.; Shreve, A. P.; Lindsey, J. S.; Donohoe, R. J. *J. Phys. Chem. B* **1998**, *102*, 4209−4216.

(53) Gaab, K. M.; Bardeen, C. J. *J. Chem. Phys.* **2004**, *121*, 7813−7820.

(54) Lahiri, S.; Thompson, J. L.; Moore, J. S. *J. Am. Chem. Soc.* **2000**, *122*, 11315−11319.

(55) Hill, D. J.; Moore, J. S. *Proc. Natl. Acad. Sci. U.S.A.* **2002**, *99*, 5053−5057.

(56) Martinho, J. M. G. *J. Phys. Chem.* **1989**, *93*, 6687−6692.

(57) Ferrante, C.; Kensy, U.; Dick, B. *J. Phys. Chem.* **1993**, *97*, 13457−13463.

(58) Knox, R. S.; Amerongen, H. v. *J. Phys. Chem. B* **2002**, *106*, 5289−5293.

(59) Monshouwer, R.; Abrahamsson, M.; Mourik, F. v.; Grondelle, R. v. *J. Phys. Chem. B* **1997**, *101*, 7241−7248.

(60) Hirata, Y.; Okada, T.; Mataga, N.; Nomoto, T. *J. Phys. Chem.* **1992**, *96*, 6559−6563.

(61) Hirata, Y. *Bull. Chem. Soc. Jpn.* **1999**, *72*, 1647−1664.

(62) Zimdars, D.; Francis, R. S.; Ferrante, C.; Fayer, M. D. *J. Chem. Phys.* **1997**, *106*, 7498−7511.

(63) Brizius, G.; Billingsley, K.; Smith, M. D.; Bunz, U. H. F. *Org. Lett.* **2003**, *5*, 3951−3954.

(64) Devadoss, C.; Bharathi, P.; Moore, J. S. *Angew. Chem., Int. Ed. Engl.* **1997**, *36*, 1633−1635.

(65) Hindin, E.; Forties, R. A.; Loewe, R. S.; Ambroise, A.; Kirmaier, C.; Bocian, D. F.; Lindsey, J. S.; Holten, D.; Knox, R. S. *J. Phys. Chem. B* **2004**, *108*, 12821−12832.

(66) Raychaudhuri, S.; Shapir, Y.; Chernyak, V.; Mukamel, S. *Phys. Rev. Lett.* **2000**, *85*, 282−285.

(67) Raychaudhuri, S.; Shapir, Y.; Mukamel, S. *Phys. Rev. E* **2002**, *65*, 021803.

(68) Krueger, B. P.; Scholes, G. D.; Fleming, G. R. *J. Phys. Chem. B* **1998**, *102*, 5378−5386.

(69) Ortiz, W.; Krueger, B. P.; Kleiman, V. D.; Krause, J. L.; Roitberg, A. E. *J. Phys. Chem. B* **2005**, *109*, 11512−11519.

(70) Grage, M. M.-L.; Wood, P. W.; Ruseckas, A.; Pullerits, T.; Mitchell, W.; Burn, P. L.; Sundstrom, V. *J. Chem. Phys.* **2003**, *118*, 7644−7650.

(71) Beenken, W. J. D.; Pullerits, T. *J. Chem. Phys.* **2004**, *120*, 2490−2495.